Nanostructures

DOI: 10.1002/anie.201201973

How Water Dissolves in Protic Ionic Liquids**

*Robert Hayes, Silvia Imberti, Gregory G. Warr, and Rob Atkin**

In recent years, ionic liquids (ILs) have emerged as useful chemical solvents for an enormous number of processes and technologies.[1,2] Their ions have more complex chemical structures than inorganic salts; by incorporating large, sterically mismatched anions and cations, ILs melt at low temperatures because, compared to typical inorganic salts, Coulombic attractions are weakened and lattice-packing arrangements frustrated.[3] ILs are regarded as "designer solvents", as molecular control over liquid properties is possible depending on how the ions are functionalized. Hydrogen bonding can play a key role in IL chemistry.[4–6] Whereas most inorganic salts cannot form hydrogen bonds and are dominated by electrostatic interactions between ions, many ILs have extensive H-bonding capacity. For example, H-bond donor and acceptor sites are created during synthesis of protic ionic liquids (PILs).[2] This enables some PILs to develop dense H-bond networks and thus mirrors a number of remarkable structural[5] and solvent[2] properties of water. Finally, ILs have the capacity to self-assemble, forming well-defined nanostructures in the bulk phase[7–13] as well as at interfaces.[3,14–16] IL nanostructure arises because at least one of the ions (frequently the cation) is amphiphilic, with distinct charged and uncharged moieties.[9] This drives segregation of ionic and nonionic groups in ILs, reminiscent of self-assembly in aqueous surfactant mesophases.[3,12]

Here we elucidate the bulk solvent structure of mixtures of a PIL, ethylammonium nitrate (EAN), and water (Figure 1). EAN is one of the oldest known[17] and most extensively studied PILs. As EAN is completely miscible with water, this raises questions such as: how do EAN and water mix? Are the forces that lead to self-assembly in pure EAN[9] sufficient to maintain a solvophobic nanostructure? What is the nature of ion solvation in such mixtures? If nanostructure persists in aqueous mixtures and key solvent properties are retained, this will increase PIL utility by offering an additional mechanism for tuning liquid behavior and lowering the overall cost of the solvent medium.

[*] R. Hayes, Dr. R. Atkin
Discipline of Chemistry, The University of Newcastle
Callaghan, NSW 2308 (Australia)
Dr. S. Imberti
STFC, Rutherford Appleton Laboratory
Didcot (UK)
Prof. G. G. Warr
School of Chemistry, The University of Sydney
Sydney, NSW 2006 (Australia)

[**] This research was supported by an ARC Discovery Project (grant number DP0986194), the AMRFP, and an ISIS beamtime grant (grant number RB820100). The authors thank Dr. Alan Soper for the H_2O $g(r)$ data. R.H. thanks the AINSE for a PGRA.

Supporting information for this article is available on the WWW under http://dx.doi.org/10.1002/anie.201201973.

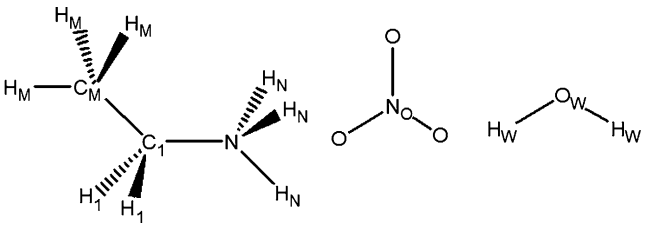

Figure 1. Molecular structure and atom types of the ethylammonium (EA^+) cation, nitrate (NO_3^-) anion, and water molecule. Different C, N, O, and H atoms are distinguished using subscripts.

While primitive (continuum solvent) models of dilute aqueous electrolyte solutions are generally successful, understanding ion–water interactions and concentrated solutions has proved challenging, and is complicated in part by the absence of a satisfactory model for liquid water.[18,19] The structure in aqueous electrolyte solutions is understood in terms of Hofmeister[20] and hydrophobic[21] effects, which can only be probed using sophisticated experimental[22–24] and computational[25–27] techniques. Solvated ions induce a different local structure of water molecules in the first, and even the second or third solvation shells, to accommodate the dissolved species. This leads to ions being classified as either "structure making" or "structure breaking" through the creation of "solute cavities".[28]

Recent, growing interest in IL/water mixtures has been motivated, at least in part, by the desire to understand the dramatic changes in IL solvent properties observed upon water contamination.[29] Water is probably the most common impurity in ILs; even nominally hydrophobic ILs absorb significant quantities of water when exposed to the atmosphere.[30] Many computational models have been developed that examined changes in IL solvent structure by dissolved water, often over the full concentration range.[31–35] At low water concentration, the models predict that the IL nanostructure is relatively unperturbed, but at high water content the system resembles aqueous solutions of ionic surfactants. However, these studies have overwhelmingly investigated aprotic ILs; largely absent are corresponding studies of PILs and experimental verification of the findings. Only one paper[11] has directly investigated the structure of PIL/water mixtures. Small- and wide-angle X-ray scattering (SWAXS) was used to investigate the effect of water on a range of PILs. For neat PILs like EAN, the SWAXS spectra were consistent with nanoscale structure, and were essentially invariant with increasing water content. A micelle-like model was proposed for the solution structure, with water located in the bulk polar domains and associated with the charge groups on the ions.

Figure 2 shows the neutron diffraction data and EPSR[36] fits to the three EAN/water mixtures in a molar ratio of 1:6 for different neutron contrasts ($[D_3]EAN + D_2O$, $[D_8]EAN +$

© 2012 Wiley-VCH Verlag GmbH & Co. KGaA, Weinheim

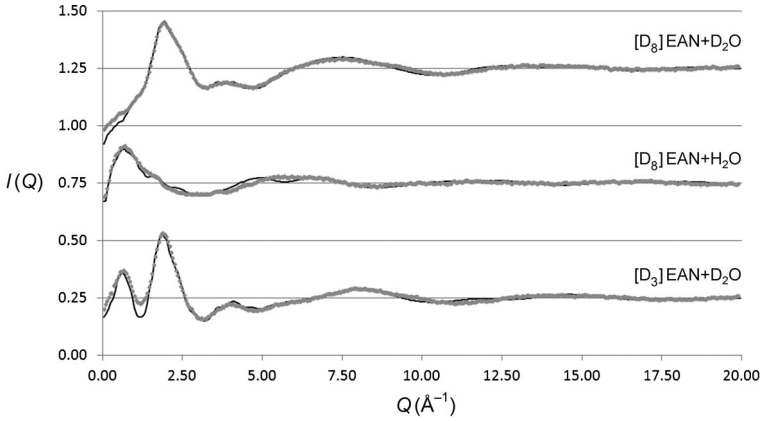

Figure 2. Experimental (dots) and EPSR-fitted (solid line) scattered intensity as a function of Q ($Å^{-1}$) for EAN/water mixtures in a molar ratio of 1:6 at 298 K; $[D_3]EAN + D_2O$ (bottom), $[D_8]EAN + H_2O$ (middle), $[D_8]EAN + D_2O$ (top). Data for different isotopic substitutions are offset for clarity.

H_2O, and $[D_8]EAN + D_2O$). Excellent agreement is obtained across the entire angular (Q-)range. The data closely resemble those previously obtained on the same instrument for different isotopomers of pure EAN.[9] Notably, a sharp peak is detected at low ($< 1\ Å^{-1}$) angles, as previously reported in neutron[8,9] and X-ray[11,37] scattering for pure EAN and EAN/H_2O mixtures,[11] but is absent in pure water or other similar molecular solvents. This indicates that a repeat distance of 10.1 Å is present in the bulk solution.

Figures 3 and 4 show atom–atom partial radial distributions, $g(r)$, and their corresponding 3D reconstructed spatial density functions (sdf) for key-selected atomic species in these mixtures. A more complete set of $g(r)$ distributions, sdf plots as well as their coordination numbers from the EAN/water mixture are provided in the Supporting Information.

The main ion–ion pair correlation functions are presented in Figure 3A and compared with our previous results for pure EAN.[9] The peak position for the anion–cation (N_O-N) correlation is very similar to pure EAN but slightly narrower and shifted to slightly smaller separation. Conversely, nearest-neighbor correlations between anions (N_O-N_O), the charged part of the cation (N-N), and the uncharged part of the cation (C_M-C_M) are weaker in the EAN/water mixture than in pure EAN. The strong cation–anion (N_O-N) correlation peak and the persistence of the low-angle scattering peak are both inconsistent with simple dilution of ions by water. Thus, water must change the liquid nanostructure but not destroy it; the EAN/water mixtures are not an unstructured homogenous solution.

The EPSR-derived spatial density plots (Figure 3C–F) show the most probable 3D arrangement of ions around the

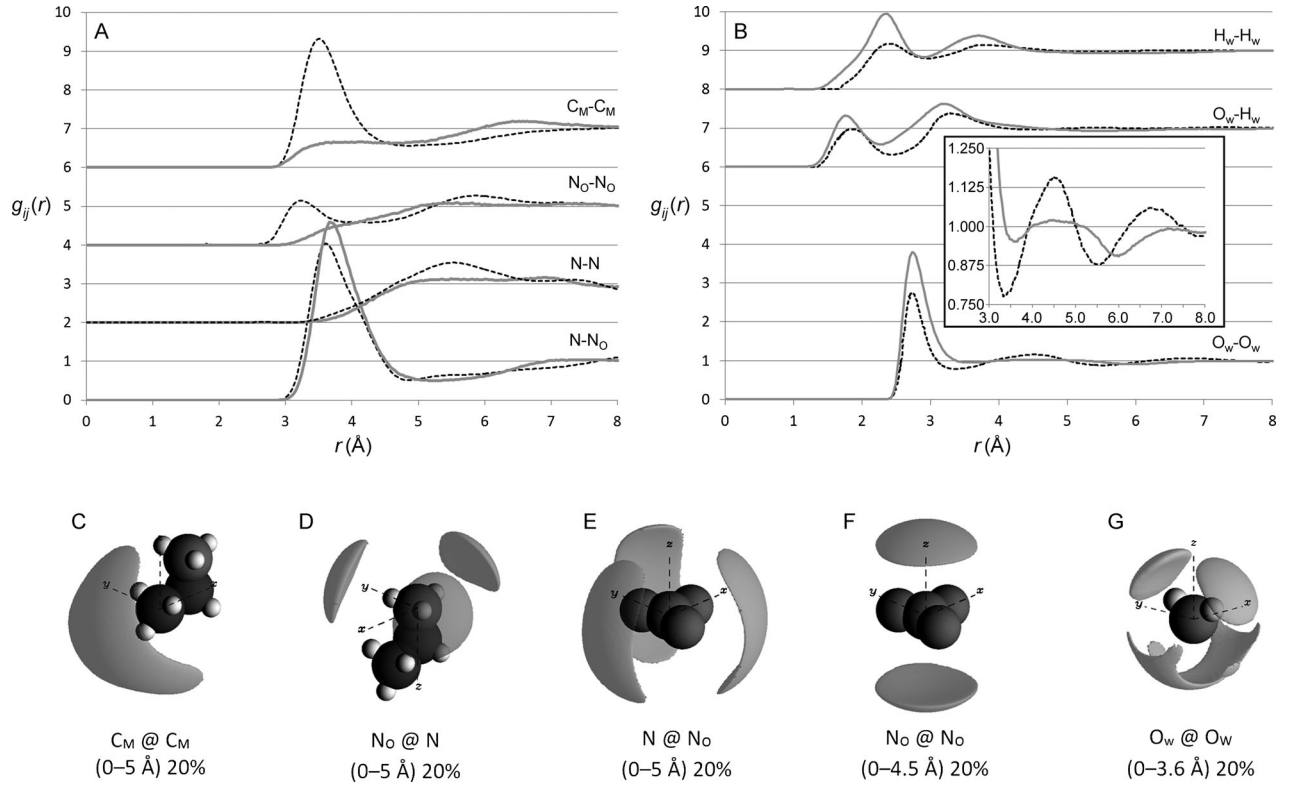

Figure 3. EPSR-derived data for key atom–atom pair correlations in A) EAN-EAN and B) H_2O-H_2O. $g(r)$ data for pure H_2O and pure EAN is shown as black dots sourced from Refs. [9] and [22]. The intensities are offset for clarity. The inset shows a close-up of the O_w-O_w $g(r)$ between 3.0–8.0 Å. C–G) EPSR sdf plots which show 3D reconstructions of $g(r)$ data. The sdf legends indicate 20% probability surfaces of $atom_1$ ordering around $atom_2$ between the given radial limits.

 © 2012 Wiley-VCH Verlag GmbH & Co. KGaA, Weinheim

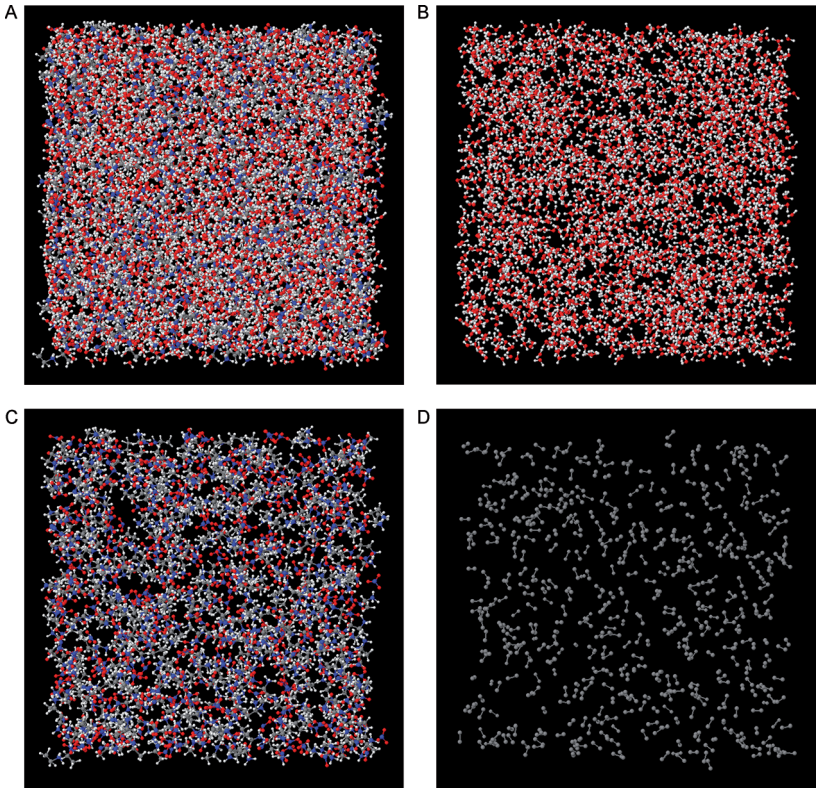

Figure 4. Snapshots of the fitted EAN + H_2O bulk structure at 298 K: A) 500 EA^+, 500 NO_3^-, and 3000 H_2O, B) 3000 H_2O (ions omitted), C) 500 EA^+ and 500 NO_3^- (water omitted), and D) apolar -C-C- domains only (-NH_3^+, NO_3^-, and H_2O omitted). C is grey, H is white, N is blue, and O is red. The $g(r)$ data and sdf plots are derived from averaging the local ion environments present in over 5000 of such equilibrated simulation boxes.

ethylammonium (3C,D) and nitrate (3E,F) ions in EAN/water mixtures. The arrangement of cations around anions (and vice versa) shown in Figure 3D and E is virtually identical to that determined previously for pure EAN, as would be expected from the similarity in the N-N_O $g(r)$ data. Figure 3C shows the position of the cation methyl carbon atoms. While the C_M-C_M $g(r)$ data show that fewer C_M atoms are present in the first C_M solvation shell, their arrangement is similar to that found in pure EAN. This shows that the key interactions driving bulk PIL nanostructure are maintained on dilution; solvophobic aggregation of cation alkyl chains as well as Coulombic and H-bonding attraction forces between ammonium moiety and nitrate ions are still clearly evident, leading to a local apolar and polar domain structure in the EAN/H_2O mixture.

Strikingly, the water–water structure differs little from that determined from scattering studies of pure water. In Figure 3B, correlation peaks can be identified in the mixture at 2.3 and 3.7 Å for H_W-H_W (2.4 and 3.7 Å in pure water) and 1.8 and 3.2 Å for O_W-H_W (1.8 and 3.3 Å).[18] Of greater significance is the O_W-O_W $g(r)$, which has been the traditional yardstick for comparing models of water. The mixture shows a sharp peak at 2.8 Å, in perfect agreement with scattering from pure water at ambient temperatures,[18] and consistent with previous findings that the nearest-neighbor O_W-O_W distance is not affected by dissolved ions.[22,23] At larger separations, the O_W-O_W $g(r)$ shows two broader, weaker correlations at approximately 4.4 and 7.1 Å (see Figure 3B inset). That the peak at 4.4 Å is so close to its pure water counterpart at 4.5 Å[18] is remarkable, as this is characteristic of the tetrahedral H-bonding network in water. For inorganic salt solutions, this peak moves inwards to shorter distances with increasing ion concentrations,[22,23,26] becoming a shoulder on the first peak at similar ion concentrations to the present study, indicating a distorted H-bond network. Instead, Figure 3B shows a decrease in peak amplitude, but with a miniscule inward shift. These results imply that the second water shell has not collapsed into the first and that the essential features of the bulk H-bond network of water are retained in the EAN/water mixture. The distinctly tetrahedral appearance of the sdf plot (Figure 3G) supports this conclusion and is also perfectly analogous to pure bulk water.[18,19]

How can this mixture support two local microenvironments so similar to the pure liquid components? Figure 4A–D shows four representations of a single fitted, equilibrated simulation box. The structure is bicontinuous, as per pure EAN, with cation ethyl groups (Figure 4D) clearly clustered together and separated from each other by intervening polar regions. However in the water (Figure 4B) and EAN (Figure 4C) snapshots, separate EAN and H_2O domains are also evident. This is a significant departure from traditional ion–water interactions at high concentrations as the ions are segregated from the water phase but are still completely miscible because ion self-assembly occurs in a fashion similar to surfactant solutions, but on a length scale an order of magnitude smaller.[3] This means that a well-defined interface must exist in the liquid mixture, consisting of the nonpolar ethyl groups on one side, and amino cation, nitrate anion, and water on the other side.

In the polar domains, local structures closely resembling pure water and pure EAN correlations arise, confirming that these interactions are unaffected by mixing. However, correlations between like groups (anions, cation charged group, cation uncharged group) are reduced because of cation–H_2O and anion–H_2O correlations. Because water is principally associated with the charged groups on the ions, its net effect is to increase the effective head group size of the cation, which raises the interfacial curvature around the nonpolar regions. This changes the EAN nanostructure from a near-zero mean curvature, or locally flat L_3-sponge-like in pure EAN,[9] to a branched (locally cylindrical) network or mesh[38] in EAN/water mixtures.

A higher curvature network structure accounts for the similarity in the EAN ion pair arrangements, the reduction in correlations between like species, and the preservation of solvophobic interactions that produce liquid nanostructures.

 © 2012 Wiley-VCH Verlag GmbH & Co. KGaA, Weinheim

Water neither simply dilutes the molecularly dispersed ions of an IL, nor does it just swell the polar region of the existing IL nanostructure. Instead, interactions between water and the charged groups of the IL change the curvature of the interface, transforming it into a related, but different nanostructure. This reveals yet another unanticipated example of the amphiphilicity of EAN, and of the rich structural polymorphism in ILs and their mixtures.

Experimental Section

The chemically identical, but isotopically different samples of EAN were prepared as described previously.[9] Solutions of EAN/H_2O in a molar ratio of 1:6 were then prepared by mixing the pure EAN isotopomers with either reverse osmosis (RO) water or fresh deuterium oxide, D_2O (99% Sigma Aldrich). Neutron diffraction data were collected on the SANDALS diffractometer (Q range 0.05–50 $Å^{-1}$) located at the ISIS research facility, Rutherford Appleton Laboratories, UK. All other experimental details, including protocols of Gudrun data normalization, can be found in Ref. [9].

Data fitting was performed using Empirical Potential Structure Refinement (EPSR).[36] In this study, the simulation box consisted of 3000 H_2O molecules and 500 EAN ion pairs, with the reference pair interaction potential defined using the values in Table S1 (see the Supporting Information).

Received: March 13, 2012
Revised: May 29, 2012
Published online: June 13, 2012

Keywords: ionic liquids · hydrogen bonds · nanostructures · self-assembly · water

[1] J. P. Hallett, T. Welton, *Chem. Rev.* **2011**, *111*, 3508.
[2] T. L. Greaves, C. J. Drummond, *Chem. Rev.* **2008**, *108*, 206–237.
[3] R. Hayes, G. G. Warr, R. Atkin, *Phys. Chem. Chem. Phys.* **2010**, *12*, 1709–1723.
[4] C. Roth, T. Peppel, K. Fumino, M. Köckerling, R. Ludwig, *Angew. Chem.* **2010**, *122*, 10419–10423; *Angew. Chem. Int. Ed.* **2010**, *49*, 10221–10224.
[5] K. Fumino, A. Wulf, R. Ludwig, *Angew. Chem.* **2009**, *121*, 3230; *Angew. Chem. Int. Ed.* **2009**, *48*, 3184.
[6] K. Fumino, A. Wulf, R. Ludwig, *Phys. Chem. Chem. Phys.* **2009**, *11*, 8790–8794.
[7] Y. Wang, G. A. Voth, *J. Am. Chem. Soc.* **2005**, *127*, 12192–12193.
[8] R. Atkin, G. G. Warr, *J. Phys. Chem. B* **2008**, *112*, 4164–4166.
[9] R. Hayes, S. Imberti, G. G. Warr, R. Atkin, *Phys. Chem. Chem. Phys.* **2011**, *13*, 3237–3247.
[10] R. Hayes, S. Imberti, G. G. Warr, R. Atkin, *Phys. Chem. Chem. Phys.* **2011**, *13*, 13544.
[11] T. L. Greaves, D. F. Kennedy, A. Weerawardena, N. M. K. Tse, N. Kirby, C. J. Drummond, *J. Phys. Chem. B* **2011**, *115*, 2055.
[12] O. Russina, A. Triolo, L. Gontrani, R. Caminiti, *J. Phys. Chem. Lett.* **2011**, *2*, 27–33.
[13] C. Hardacre, J. D. Holbrey, C. L. Mullan, T. G. A. Youngs, D. T. Bowron, *J. Chem. Phys.* **2010**, *133*, 074510.
[14] T. Yan, S. Li, W. Jiang, X. P. Gao, B. Xiang, G. A. Voth, *J. Phys. Chem. B* **2006**, *110*, 1800–1806.
[15] W. Jiang, Y. Wang, T. Yan, G. A. Voth, *J. Phys. Chem. C* **2008**, *112*, 1132–1139.
[16] R. Hayes, N. Borisenko, M. K. Tam, P. C. Howlett, F. Endres, R. Atkin, *J. Phys. Chem. C* **2011**, *115*, 6855–6863.
[17] P. Walden, *Bull. Acad. Imp. Sci.* **1914**, 1800.
[18] T. Head-Gordon, G. Hura, *Chem. Rev.* **2002**, *102*, 2651.
[19] A. K. Soper, *Pure Appl. Chem.* **2010**, *82*, 1855.
[20] D. F. Parsons, M. Boström, P. Lo Nostroc, B. W. Ninham, *Phys. Chem. Chem. Phys.* **2011**, *13*, 12352.
[21] E. Meyer, K. J. Rosenberg, J. Israelachvili, *Proc. Natl. Acad. Sci. USA* **2006**, *103*, 15739.
[22] R. Mancinelli, A. Botti, F. Bruni, M. A. Ricci, A. K. Soper, *Phys. Chem. Chem. Phys.* **2007**, *9*, 2959.
[23] R. Mancinelli, A. Botti, F. Bruni, M. A. Ricci, A. K. Soper, *J. Phys. Chem. B* **2007**, *111*, 13570.
[24] A. W. Omta, M. F. Kropman, S. Woutersen, H. J. Bakker, *Science* **2003**, *301*, 347.
[25] B. Hribar, N. T. Southall, V. Vlachy, K. A. Dill, *J. Am. Chem. Soc.* **2002**, *124*, 12302.
[26] J. Holzmann, R. Ludwig, A. Geiger, D. Paschek, *Angew. Chem.* **2007**, *119*, 9065; *Angew. Chem. Int. Ed.* **2007**, *46*, 8907.
[27] F. Jalilehvand, D. Spångberg, P. Lindqvist-Reis, K. Hermansson, I. Persson, M. Sandström, *J. Am. Chem. Soc.* **2001**, *123*, 431.
[28] Y. Marcus, *Chem. Rev.* **2009**, *109*, 1346–1370.
[29] F. Endres, S. Zein El Abedin, *Phys. Chem. Chem. Phys.* **2006**, *8*, 2101–2116.
[30] F. D. Francesco, N. Calisi, M. Creatini, B. Melai, P. Salvo, C. Chiappe, *Green Chem.* **2011**, *13*, 1712–1717.
[31] W. Jiang, Y. Wang, G. A. Voth, *J. Phys. Chem. B* **2007**, *111*, 4812–4818.
[32] C. E. S. Bernardes, M. E. Minas da Piedade, J. N. Canongia Lopes, *J. Phys. Chem. B* **2011**, *115*, 2067–2074.
[33] B. L. Bhargava, Y. Yasaka, M. L. Klein, *Chem. Commun.* **2011**, *47*, 6228–6241.
[34] S. Zahn, K. Wendler, L. Delle Site, B. Kirchner, *Phys. Chem. Chem. Phys.* **2011**, *13*, 15083–15093.
[35] S. Feng, G. A. Voth, *Fluid Phase Equilib.* **2010**, *294*, 148–156.
[36] A. K. Soper, *Phys. Rev. B* **2005**, *72*, 104204.
[37] Y. Umebayashi, W. Chung, T. Mitsugi, S. Fukuda, M. Takeuchi, K. Fujii, T. Takamuku, R. Kanzaki, S. Ishiguro, *J. Comput. Chem. Jpn.* **2008**, *7*, 125.
[38] J. Burgoyne, M. C. Holmes, G. J. T. Tiddy, *J. Phys. Chem.* **1995**, *99*, 6054–6063.

 © 2012 Wiley-VCH Verlag GmbH & Co. KGaA, Weinheim